Solid-State Electronics Pergamon Press 1962. Vol. 5, pp. 341–351. Printed in Great Britain

EXPERIMENTS ON Ge–GaAs HETEROJUNCTIONS

R. L. ANDERSON*

International Business Machines Corporation, Yorktown Heights, New York

(*Received* 29 *January*; *in revised form* 23 *April* 1962)

Abstract—The electrical characteristics of Ge–GaAs heterojunctions, made by depositing Ge epitaxially on GaAs substrates, are described. *I–V* and electro-optical characteristics are consistent with a model in which the conduction- and valence-band edges at the interface are discontinuous. The forbidden band in heavily doped (*n*-type) germanium appears to shift to lower energy values.

Résumé—Les caractéristiques électriques des hétérojunctions de Ge–GaAs produites en déposant le Ge épitaxiallement sur les couches inférieures de l'AsGa sont décrites. Les caractéristiques *I–V* et électrooptiques sont consistantes avec un modèle dans lequel les bords des bandes de conduction et de valence à l'interface sont discontinus. La bande défendue dans le germanium (type-*n*) fortement dopé semble se déplacer vers des valeurs à énergie plus basse.

Zusammenfassung—Die elektrischen Kenngrössen von Ge–GaAs Hetero-Übergängen, die man durch epitaxiale Ablagerung von Ge auf GaAs-Substraten herstellt, werden beschrieben. *I–V* und elektro-optische Kenndaten entsprechen einem Modell, in dem die Ränder des Leitungs- und Valenzbandes an der Grenzfläche diskontinuierlich sind. Das verbotene Band in stark dotiertem (*n*-Typ) Germanium scheint sich nach niedrigeren Energiewerten zu verlagern.

1. INTRODUCTION

JUNCTIONS between two semiconductors of the same element but with different impurities present have been studied extensively. These junctions are reasonably well understood. The periodicity of the lattice is not disturbed at the junction and so the properties of the semiconductors at the junction can be expected to be the bulk properties.

Metal–semiconductor contacts, on the other hand, are not well understood. The chief difficulty is usually attributed to interface effects. Even though the semiconductor and the metal may each be monocrystalline, the crystal structures and lattice constants in general are different and so an expitaxial contact is not formed. Because of the abrupt change in the structure and periodicity of the lattice and the resultant disorder in the region near the interface, material properties are not the same here as they are in the bulk.

The theoretical voltage–current characteristic of a *p–n* junction or a metal semiconductor contact is derived for most models to be of the form[1]

$$I = I_0[\exp(qV/kT)-1] \qquad (1)$$

where I is the current due to an applied voltage V, I_0 is the saturation current or the current for large negative voltage, q is the electronic charge, k is Boltzmann's constant and T is the absolute temperature. The value of I_0 is reasonably independent of voltage in most derivations. The diode formula is often written in the form

$$I = I_0[\exp(qV/\eta kT)-1] \qquad (2)$$

where η is an empirical factor which describes the disagreement between simple theory and experiment for forward bias ($V > 0$). The value of η is commonly about 2·3 for gallium arsenide *p–n* junctions, is between 2 and 4 in Ge point-contact diodes and approaches the theoretical value of unity only in Ge *p–n* junctions (and in silicon *p–n* junctions at elevated temperatures). The variation of current with reverse voltage is usually accounted for by permitting the term I_0 to vary slowly with voltage. These deviations from the theory have not been adequately explained.

* Now at the Department of Electrical Engineering, Syracuse University, Syracuse, New York.

Little work has been done on junctions between two semiconductors. GUBANOV has suggested that the I–V characteristics of copper oxide rectifiers might be indicative of semiconductor–semiconductor contacts.* SHOCKLEY[3] and KRÖMER[4] suggested using a semiconductor with a wide forbidden region as an emitter for a transistor which has base and collector of a narrower-gap semiconductor. The purpose of this is to obtain a high injection efficiency. JENNY[5] has described attempts to fabricate a GaP–GaAs wide-gap emitter by diffusing phosphorus into gallium arsenide. Little success has been reported.

This paper discusses the electrical characteristics of junctions formed between Ge and GaAs. These junctions are contained within a monocrystal. Ge was deposited epitiaxially onto GaAs seeds by the Iodide Process.[6–8] These two materials have similar crystal structure, and virtually equal lattice constants (5·62 Å). As a result, it is expected that strain at the interface is negligible.

Junctions between two dissimilar materials will be referred to as "heterojunctions" in contrast to "homojunctions" where only one semiconductor is involved.

2. ENERGY-BAND PROFILE OF HETERO-JUNCTIONS

Consider the energy-band profile of two isolated pieces of semiconductor shown in Fig. 1. The two semiconductors are assumed to have different band gaps (E_g), different dielectric constants (ϵ), different work functions (ϕ) and different electron affinities (θ). Work function and electron affinity are defined, respectively, as that energy required to remove an electron from the Fermi level (E_f) and from the bottom of the conduction band (E_c) to a position just outside of the material (vacuum level). The top of the valence band is represented by E_v. The subscripts 1 and 2 refer to the narrow-gap and wide-gap semiconductors, respectively.

In Fig. 1, the band-edge profiles (E_{c1}, E_{c2}, E_{v1}, E_{v2}) are shown to be "horizontal". This is equivalent to assuming that space-charge neutrality exists in every region. The difference in energy of the conduction-band edges in the two materials is represented by ΔE_c and that in the valence-band edges by ΔE_v.

* For a review of Gubanov's work see Ref. 2.

A junction formed between an n-type narrow-gap semiconductor and a p-type wide-gap semiconductor is considered first. This is referred to

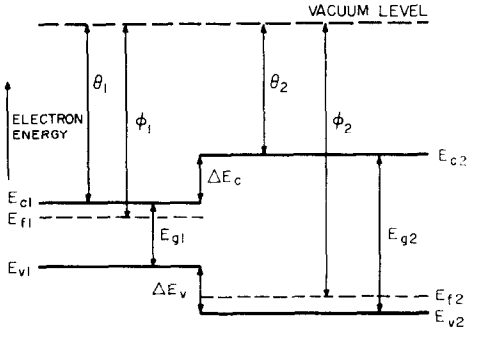

FIG. 1. Energy-band diagram for two isolated semiconductors in which space-charge neutrality is assumed to exist in every region.

as an n–p heterojunction. The energy-band profile of such a junction at equilibrium is shown in Fig. 2.

Within any single semiconductor the electrostatic potential difference between any two points

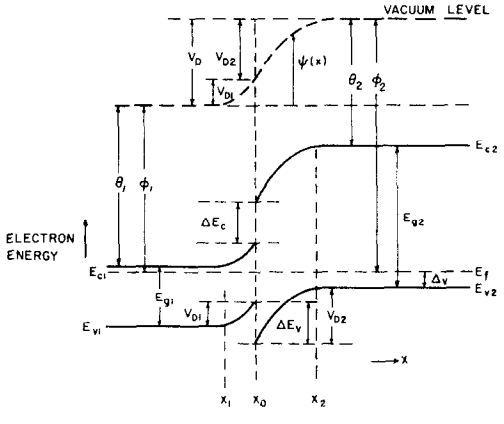

FIG. 2. Energy-band diagram of n–p heterojunction at equilibrium.

can be represented by the vertical displacement of the band edges between these two points, and the electrostatic field can be represented by the slope of the band edges on a diagram such as Fig. 2. Then the difference in the work functions of the two materials is the total built-in voltage (V_D). V_D is equal to the sum of the partial built-in

voltages ($V_{D1}+V_{D2}$) where V_{D1} and V_{D2} are the electrostatic potentials supported at equilibrium by semiconductors 1 and 2, respectively. Since voltage is continuous in the absence of dipole layers, and since the vacuum level is parallel to the band edges, the electrostatic potential difference (ψ) between any two points is represented by the vertical displacement of the vacuum level between these two points. Because of the difference in dielectric constants in the two materials, the electrostatic field is discontinuous at the interface.

Since the vacuum level is everywhere parallel to the band edges and is continuous, the discontinuity in conduction-band edges (ΔE_c) and valence-band edges (ΔE_v) is invariant with doping in those cases where the electron affinity and band gap (E_g) are not functions of doping (i.e. nondegenerate material).

Solutions to Poisson's equation, with the usual assumptions of a Schottky barrier,* give, for the transition widths on either side of the interface for a step junction,

$$(X_0-X_1)=\left[\frac{2}{q}\frac{N_{A2}\epsilon_1\epsilon_2(V_D-V)}{N_{D1}(\epsilon_1N_{D1}+\epsilon_2N_{A2})}\right]^{1/2} \quad (3a)$$

$$(X_2-X_0)=\left[\frac{2}{q}\frac{N_{D1}\epsilon_1\epsilon_2(V_D-V)}{N_{A2}(\epsilon_1N_{D1}+\epsilon_2N_{A2})}\right]^{1/2} \quad (3b)$$

and the total width W of the transition region is

$$W=(X_2-X_0)+(X_0-X_1)$$

$$=\left[\frac{2\epsilon_1\epsilon_2(V_D-V)(N_{A2}+N_{D1})^2}{(q\epsilon_1N_{D1}+\epsilon_2N_{A2})N_{D1}N_{A2}}\right]^{1/2} \quad (4)$$

The relative voltages supported in each of the semiconductors are

$$\frac{V_{D1}-V_1}{V_{D2}-V_2}=\frac{N_{A2}\epsilon_2}{N_{D1}\epsilon_1} \quad (5)$$

where V_1 and V_2 are the portions of the applied voltage V supported by materials 1 and 2 respectively. Of course $V_1+V_2=V$. Then $(V_{D1}-V_1)$ and $(V_{D2}-V_2)$ are the total voltages (built in plus applied) for material 1 and material 2, respectively. We can see that most of the potential difference occurs in the most lightly doped region for nearly equal dielectric constants.

The transition capacitance is given by a generalization of the result for homojunctions:

$$C=\left[\frac{qN_{D1}N_{A2}\epsilon_1\epsilon_2}{2(\epsilon_1N_{D1}+\epsilon_2N_{A2})}\frac{1}{(V_D-V)}\right]^{1/2} \quad (6)$$

It can be seen from Fig. 2 that the barrier to electrons is considerably greater than that to holes, and so hole current will predominate.

The case of an n–n junction of the above two materials is somewhat different. Since the work function of the wide-gap semiconductor is the smaller, the energy bands will be bent oppositely to the n–p case (See Fig. 3). However, there are

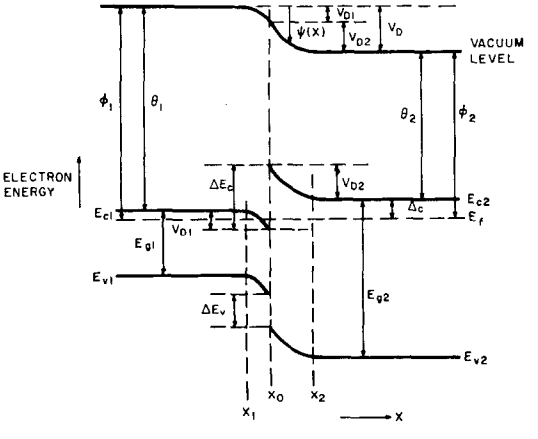

FIG. 3. Energy-band diagram of n–n heterojunction at equilibrium.

a negligible number of states available in the valence band and so the excess electrons in the material of greater work function will occupy states in the conduction band. Since there are a large number of states available in the conduction band, the transition region extends only a small distance into the narrow-band material and the voltage is supported mainly by the material with the smaller work function.

The voltage profile in the interface region can be determined by solving for the electric field strength (F) on either side of the interface and using the condition that the electric displacement ($D=\epsilon F$) is continuous at the interface. Assuming

* See Ref. 9 for details for calculations for homojunctions.

Boltzman statistics in region 1,

$$\epsilon_1 F_1(X_0) = \left\{2\epsilon_1 q N_{D1}\left[\frac{kT}{q}\left(\exp\frac{q(V_{D1}-V_1)}{kT}-1\right)-(V_{D1}-V_1)\right]\right\}^{1/2} \quad (7)$$

In region 2 the electric displacement at the interface is

$$\epsilon_2 F_2(X_0) = [2\epsilon_2 q N_{D2}(V_{D2}-V_2)]^{1/2} \quad (8)$$

Equating equations (7) and (8) gives a relation between $(V_{D1}-V_1)$ and $(V_{D2}-V_2)$ which is quite complicated. However, it is reasonably easy to get an upper limit of $(V_{D1}-V_1)$. If the exponential in equation (1) is expanded in a Taylor series, the following inequality is obtained:

$$(V_{D1}-V_1) < \left[\frac{2kT}{q}\frac{\epsilon_2 N_{D2}}{\epsilon_1 N_{D1}}(V_{D2}-V_2)\right]^{1/2} \quad (9)$$

From equation (9) we can see that the electrostatic potential will be supported mainly by semiconductor 2 unless $N_{D2} \gg N_{D1}$, or for high forward bias.

For n–n heterojunctions the transition capacitance is difficult to calculate. However, except for the cases mentioned above, the capacitance of a metal–semiconductor contact is a good approximation.

In the heterojunctions discussed here, the energy gap of the wide-gap material (Ga–As) "overlaps" that of the narrow-gap material, and the polarity of the built-in field (and of rectification) is dependent on the conductivity type of the wide-gap semiconductor. Fig. 4 shows the equilibrium energy-band diagrams for p–n and p–p heterojunctions.

3. PREDICTED I–V CHARACTERISTICS

Because of the discontinuities in the band edges at the interface, the barriers to the two types of carriers have different magnitudes, and so current in a heterojunction will in most cases consist almost entirely of electrons or of holes.

The variation of current with applied voltage for these heterojunctions (neglecting generation–recombination current) is

$$I = A\exp(-qV_{B2}/kT) - B\exp(-qV_{B1}/kT) \quad (10)$$

where V_{B1} is the barrier that carriers in semiconductor 1 must overcome to reach semiconductor 2, and V_{B2} is the barrier to the carriers moving the opposite direction. The coefficients A and B depend on doping levels, on carrier effective mass and on the mechanism of current flow.

In the junctions depicted in Fig. 2–4, V_{B1} exists for the predominant current carrier and so

$$I = A\exp[-q(V_{D2})/kT]\,[\exp(qV_2/kT) - \exp(-qV_1/kT)] \quad (11)$$

where V_2 and V_1 are those portions of applied voltage appearing in materials 2 and 1, respectively. The first term in the brackets is important for forward bias and the second for reverse bias. If $V_2 = V/\eta$ then $V_1 = (1-1/\eta)V$ and the current varies approximately exponentially with voltage in both forward and reverse directions. It should be noticed however that at increased reverse voltage V_{B1} disappears, i.e. $(V_{D1}-V) > \Delta E_c$ (for the case of the p–n junction), and the current is expected to saturate. If $V_{D1} > \Delta E_c$ (again for a p–n heterojunction—see Fig. 5), $V_{B1} = 0$ and the

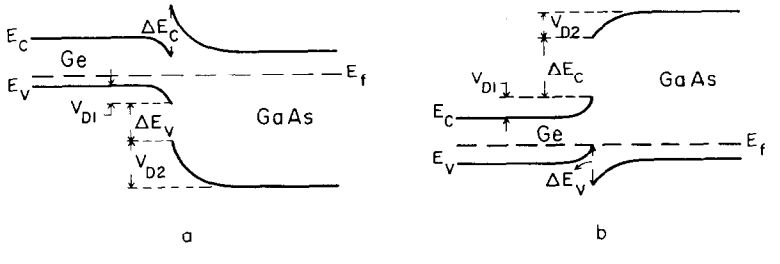

FIG. 4. Energy-band diagrams in the interface region for p–n and p–p heterojunctions. Electron energy is plotted vertically.

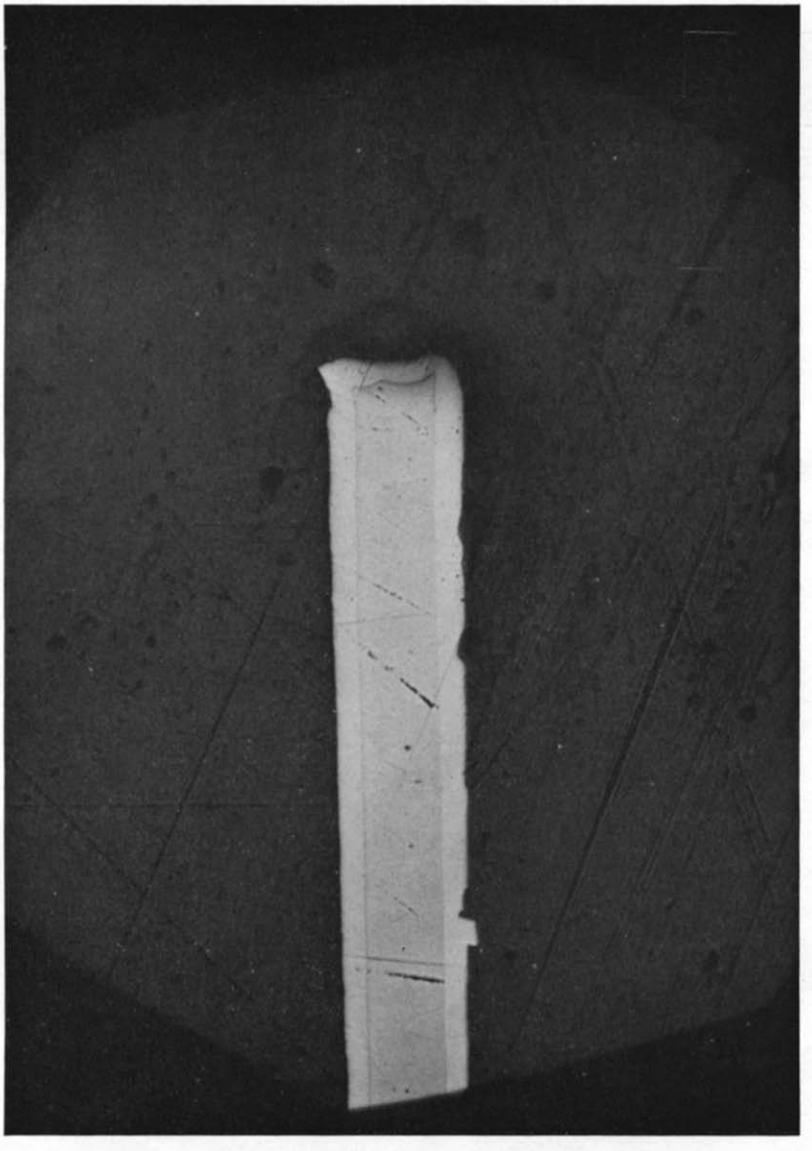

FIG. 6. Cross-sectional view of a wafer of GaAs on which Ge has been deposited. The thickness of the deposit is about 0·03 cm.

[*facing p.* 344

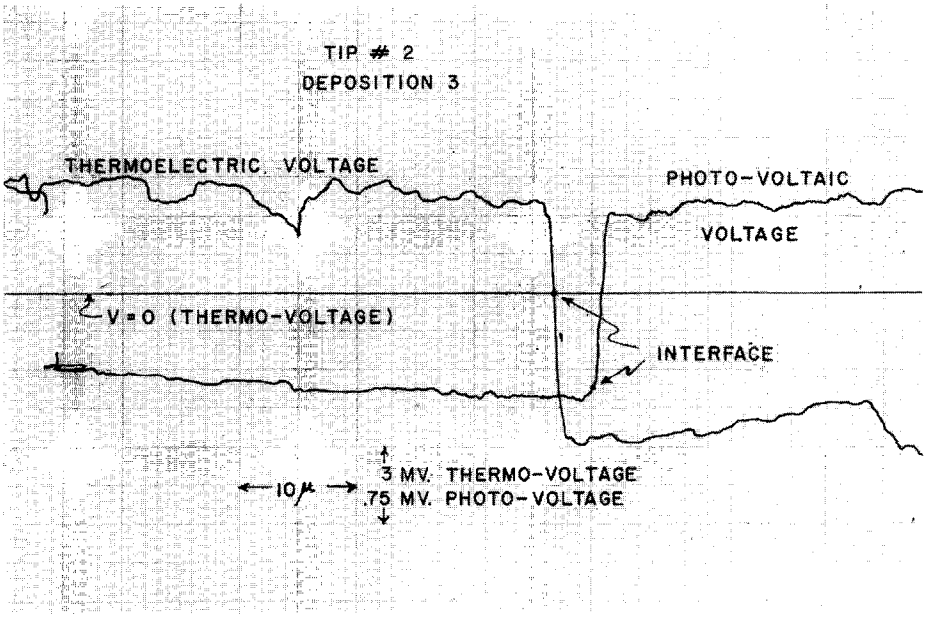

FIG. 7. Plot of photovoltage and thermoelectric voltage against distance normal to the surface for an n-p Ge–GaAs heterojunction. The surface is indicated by the extreme left of each trace. The junction position is indicated by a zero thermoelectric voltage.

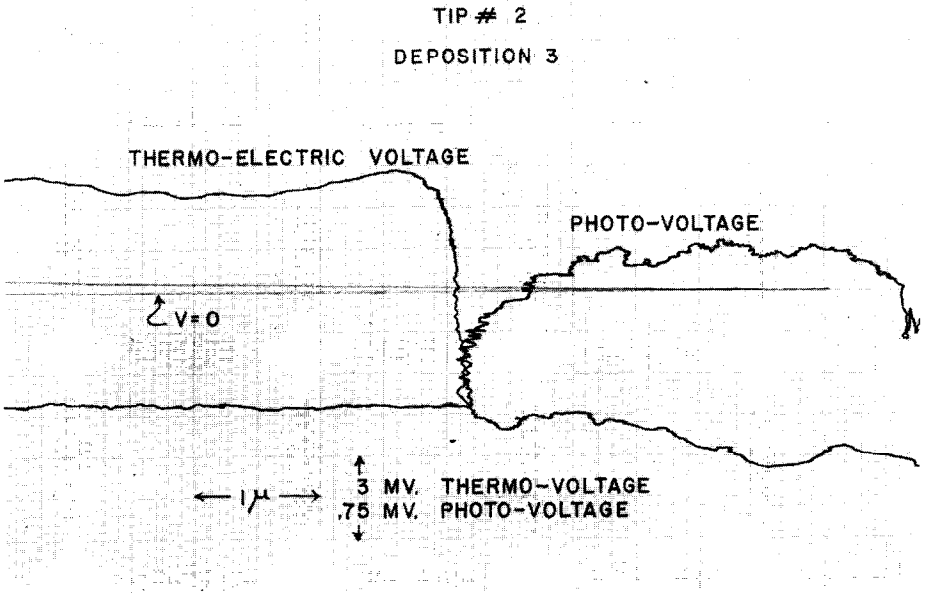

FIG. 8. Region near interface of Fig. 4 on expanded scale. The shape of the photovoltage plot indicates the transition region to be predominantly in the gallium arsenide.

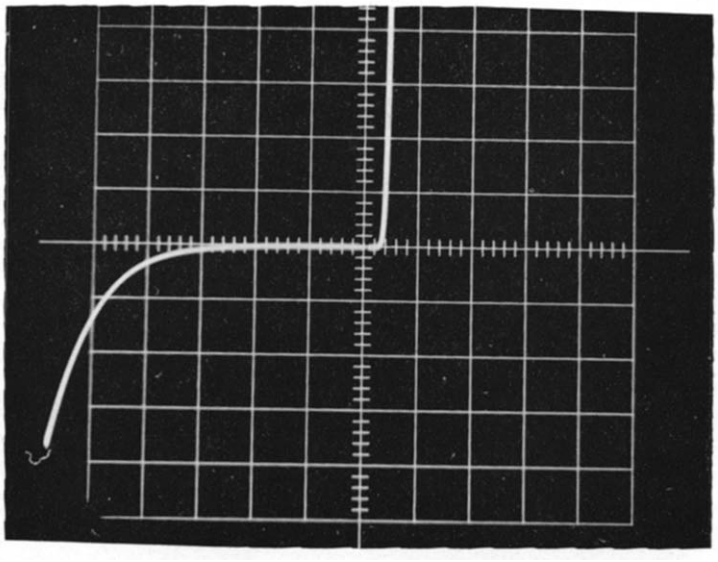

FIG. 9. V–I characteristics of a Ge–GaAs n–n heterojunction. The ordinate scale is 0·1 mA/div while the abscissa scale is 1·0 V/div.

entire applied voltage is effective in varying barrier height:

$$I = A \exp[-q(V_D - \Delta E_c)/kT][\exp(qV/kT) - 1] \quad (12)$$

Above a critical forward voltage in such a diode, V_{B1} will become finite $[(V_{D1} - V_1) < \Delta E_c]$ and the current will vary exponentially with $V_2 = V/\eta$ (see Section 4.2).

Since in the n–p heterojunction, the current is limited by the rate at which holes can diffuse in the narrow-gap material,[10]

$$A = XaqN_{A2}(D_p/\tau_p)^{1/2} \quad (13a)$$

where the transmission coefficient X represents the fraction of those carriers having sufficient energy to cross the barrier which actually do so.

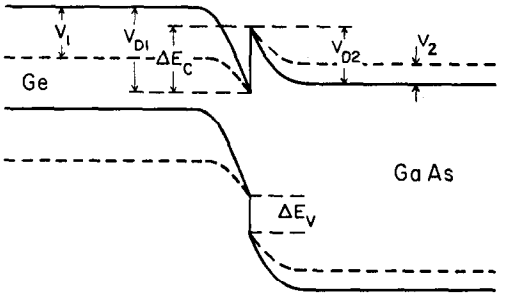

FIG. 5. Band diagram of p–n heterojunction in which no barrier exists for electrons going from Ge to GaAs (solid line) and for applied forward bias where now the barrier does exist (dashed line). The expected I–V characteristics are considerably different in the two regions.

D_p and τ_p are diffusion constant and lifetime, respectively, for holes in the narrow-gap material, and a represents junction area.

The case of the p–n heterojunction is analogous.

In the case of n–n and p–p heterojunctions, since V_{D1} and V_1 are small with respect to V_{D2} and V_2, respectively, and because the current is carried by majority carriers, we have, in analogy with the emission theory for metal–semiconductor diodes,[11]

$$A = XaqN_2\left(\frac{kT}{2\pi m^*}\right)^{1/2} \quad (13b)$$

where N_2 and m^* are, respectively, net impurity density and carrier effective mass in semiconductor 2.

The above formulae would be modified somewhat by generation–recombination[12] and "leakage" currents, by image and tunnel effects, and by interface states.

4. EXPERIMENTAL RESULTS

In this section the electrical characteristics of n–p, n–n, p–n and p–p heterojunctions are reported and interpreted with respect to the theory of Sections 2 and 3. It must be emphasized that the junctions reported here were made in two depositions. The n-type germanium in the n–p and n–n junctions is expected to be similar since this Ge (phosphorus doped) was deposited simultaneously on n- and p-type GaAs. Likewise the p-type Ge (gallium doped) in the p–n and p–p junction is expected to be similar. The p-type GaAs seeds in the n–p and p–p heterojunctions were cut from adjacent slices of a monocrystal. The same is true for the n-type GaAs seeds in the n–n and p–n junctions. Fig. 6 shows a cross-sectional view of a GaAs substrate surrounded by deposited Ge.

To fabricate a diode from such a wafer, the deposited Ge was removed from one side, and the wafer was then broken into chips. Ohmic contacts were made to both sides of the chip, and the chip was then mounted in a transistor header and etched to remove surface damage.

All heterojunctions tested showed rectification. For forward bias, the GaAs was biased negative (with respect to the Ge) for the n–n and p–n junctions and positive for n–p and p–p junctions. This is in agreement with the proposed model.

The junctions studied can be classified as being "good" diodes or "bad" diodes. The good units of each junction type all behave very nearly identically. The built-in voltages are equal and the electrical characteristics vary only slightly among units. The bad units, however, all appear to have somewhat lower built-in voltages which vary from unit to unit. Although the bad units have not been studied as intensively as the good units, it appears that if the reduced built-in voltage is taken into account, the electrical characteristics are similar to those of the good units. It is thought that the bad units contain defects at the interface which lower the barrier height. Many such bad units were transformed into good units by reducing the junction area and presumably eliminating

defects. Only the good units will be discussed further.

That rectification actually occurs at the interface was determined by probing the material.[13] Fig. 7 shows a plot of thermoelectric and of photovoltaic potential versus distance from germanium surface of an *n–p* heterojunction. The germanium surface position is represented by the extreme left of either trace. The thermoelectric voltage null is indicated to be about 46·8 μ below the germanium surface. In the photovoltage plot, the position 46·8 μ from the Ge surface is as indicated. That this position indeed corresponds to the interface can be seen from Fig. 8 where the transition region is expanded to show that the junction (position of maximum slope in the photovoltage plot) is as indicated in Fig. 7. For the case of the *n–n* or *p–p* junctions, a similar method was used. Instead of the change in polarity for the thermoelectric voltage, an abrupt change in magnitude was observed at the junction.

The deposited *n*-type Ge (in the *n–p* and *n–n* junctions) was much more heavily doped than was the GaAs. The net donor concentration in the Ge was determined by resistivity measurements and was found to be about 10^{19}/cm^3. Capacitance measurements on *n–p* and *p–p* heterojunctions indicate that the net acceptor concentration in the GaAs is constant for distance from the junction greater than 0·25 μ and is equal to $1{\cdot}5 \times 10^{16}$ atoms/cm^3. This is in agreement with Hall-effect data. In the *n–n* heterojunctions, capacity measurements indicate a net donor concentration in the GaAs varying as x[4,7] where x is the distance from the interface. At the edge of the transition region at equilibrium, the net donor concentration is about 4×10^{16} atoms/cm^3. The resistivity of the *p*-type Ge (in *p–n* and *p–p* heterojunctions) was not measured. However, electrical characteristics indicate a net acceptor concentration in the neighborhood of 10^{16} atoms/cm^3.

In the *n–n* and *p–p* junctions, the space charge in the Ge is composed of mobile carriers and so the voltage supported at the junction is expected to be almost entirely in the GaAs in these cases. However, since the *n*-type Ge is more heavily doped than the GaAs, and the *p*-type Ge is more lightly doped, the built-in voltage and transition region occur predominantly in the GaAs for *n–p* junctions and in the Ge for *p–n* junctions. This can be seen for an *n–p* junction in a plot of photo voltage *vs.* position (see Fig. 8) where the position of maximum slope indicates an undetectable voltage is supported by the Ge.

4.1 *Alignment of bands at interface*

The built-in voltages at room temperature as determined from *I–V* and from *C–V* characteristics are presented (Table 1) for representative *n–n*, *n–p*, *p–p* and *p–n* heterojunctions. The

Table 1

Heterojunction	V_D	
	I–V	*C–V*
n–n	0·47 ± 0·02	0·48 ± 0·05
n–p	0·62 ± 0·02	0·85 ± 0·05
p–p	0·56 ± 0·03	0·70 ± 0·05
p–n	0·53 ± 0·03	0·55 ± 0·05

agreement between methods is good for *n–n* and *p–n* junctions but not for *n–p* or *p–p* heterojunctions.

Since similar germanium was used for *n–n* and *n–p* junctions, the model proposed predicts that the sum of the built-in voltages (V_D) for the two types of junctions plus the energy between the appropriate band edge and the Fermi level (Δ_c, Δ_v) adds up to the band gap of the GaAs. The same is true for *p–n* and *p–p* junctions. The values of Δ_v and Δ_c are calculated to be 0·19 and 0·07 eV assuming the magnitude of the hole effective mass is equal to that of a free electron (m_0) and using the published value of $0{\cdot}078m_0$ for the electron effective mass.[14]

Then, with V_D obtained from *I–V* data,

$$0{\cdot}62+0{\cdot}47+0{\cdot}19+0{\cdot}07 = 1{\cdot}35 \text{ eV}$$

for *n–p* and *n–n* junctions and

$$0{\cdot}53+0{\cdot}56+0{\cdot}19+0{\cdot}07 = 1{\cdot}35 \text{ eV}$$

for *p–p* and *p–n* junctions, which is in good agreement with the published value of 1·36 eV for the band gap of GaAs.

The magnitude of ΔE_c and ΔE_v can be obtained only approximately from the data, because the position of the Fermi level with respect to the

conduction band edge and the band gap of this degenerate germanium can only be estimated. If the density of states in the conduction band for degenerate Ge is that for non-degenerate Ge, and if the band gap of this Ge is assumed to be 0·48 eV as suggested by PANKOVE,[15] values of 0·56 and 0·32 eV are obtained for ΔE_c and ΔE_v, respectively, for degenerate *n*-type Ge and non-degenerate GaAs.

A calculation of the band edge discontinuities for non-degenerate *p*-type Ge and non-degenerate GaAs gives values of 0·15 and 0·55 eV, respectively, for ΔE_c and ΔE_v. These measurements indicate that with increased doping of germanium with phosphorus, the entire forbidden band is depressed to lower energies.

4.2 *I–V characteristics*

The heterojunctions studied have static *I–V* characteristics reasonably typical of those reported for homojunctions. The forward current varies approximately exponentially with applied voltage, and the reverse characteristics show a soft breakdown. The *n–p* junctions show an additional abrupt breakdown which is believed to be due to the avalanche effect. Fig. 9 shows the *I–V* characteristics of an *n–n* heterojunction at room temperature.

The *I–V* characteristics can generally be written as in equation (2) where the value of η indicates the deviation from ideal forward rectifier characteristics. For *n–n* and *p–p* junctions, the applied voltage is supported almost entirely by the GaAs, and as a result the factor η is expected to approach unity. The value of η is also expected to approach unity for the *n–p* junctions, because the Ge is so much more heavily doped than is the GaAs so that again the applied voltage is almost entirely supported by the GaAs.

However, in the *p–n* heterojunctions studied, the relative dopings indicate that η should equal unity for $V_{D1} - V_1 > \Delta E_c$ and approach V/V_2 for $V_{D1} - V_1 < \Delta E_c$. The plot of $\ln I$ vs. V is shown for respective junctions of these four classes in Fig. 10. The data was taken at elevated temperatures to reduce the influence of surface leakage and generation–recombination currents.

The plots of the *n–n*, *n–p* and *p–p* junctions can all be expressed by equation (2) where η is just slightly greater than unity as is expected. The *I–V* characteristic for the *p–n* heterojunction,

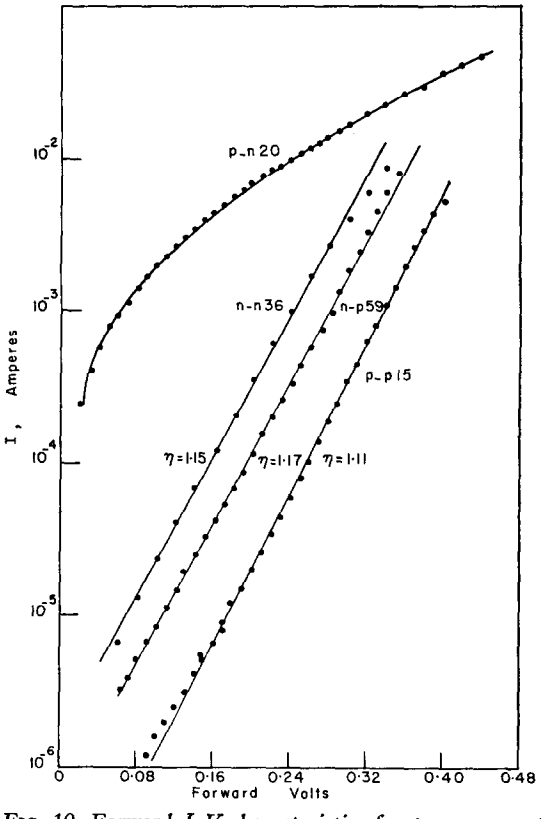

FIG. 10. Forward *I–V* characteristics for *p–n*, *n–n*, *n–p* and *p–p* heterojunctions. The indicated value of η is found by empirically fitting the expression $I = I_0 \exp(qV/\eta kT)$.

however, has a "sloppy" characteristic and a value of η of approximately 3·5, although it is not a constant. At 78°K the *I–V* characteristics of this diode are as shown in Fig. 11. There are three straight-line regions of this plot corresponding to three distinct values of η (equation 2). In region *a*, for applied voltage $V < 0{\cdot}16$ V, $\eta = 2{\cdot}1$. In the range $0{\cdot}16 < V < 0{\cdot}7$ V (region *b*), equation (2) is satisfied with $\eta = 16{\cdot}7$. For $V > 0{\cdot}7$ V (region *c*), the value of η doubles and becomes $\eta = 8{\cdot}3$. These characteristics are interpreted as follows:

The barrier is decreased by the amount of the applied voltage in region *a*. A value of $\eta = 2{\cdot}1$ results from recombination of carriers in the transition region. In regions *b* and *c*, the conduction-band edge in the Ge is lower than its

peak in the GaAs (see Fig. 5). As a result, only that portion of applied voltage (V_2) appearing in the GaAs lowers the barrier. Then effectively η is increased. The halving of η at about $V = 0{\cdot}7$ V results from the predominance of injected current above this voltage.

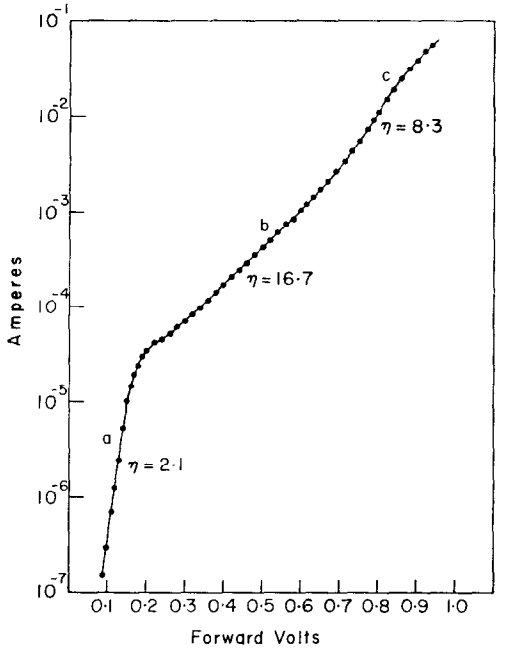

FIG. 11. Forward I–V characteristics at 78°K for p–n heterojunction having p-Ge less heavily doped than n-GaAs.

It must be pointed out that the value of ΔE_c as determined earlier would be expected to result in a change from region a to region b of the I–V characteristic at about 0·66 V, or, conversely, a value of ΔE_c of about 0·5 eV would be required to interpret the data as we have done. The reverse electrical I–V characteristics of representative n–n, n–p, p–p and p–n heterojunctions are shown in Fig. 12. Although the data was taken at elevated temperatures to minimize generation–recombination current, the reverse current does not saturate. The origin of this excess current is not known. From the magnitude of the current at a given voltage, the values of A in equations (11) and (12) can be experimentally determined. Comparing these values with equations (13a, b) give values of transmission coefficients (X) of about 10^{-3} for the n–p and p–p homojunctions, and about 10^{-6} for the n–n junction. The value of X for the p–n junction was more difficult to determine. However, a value less than 10^{-3} with a value of ΔE_c in the neighborhood of 0·5 eV seems necessary to explain the experimental results.

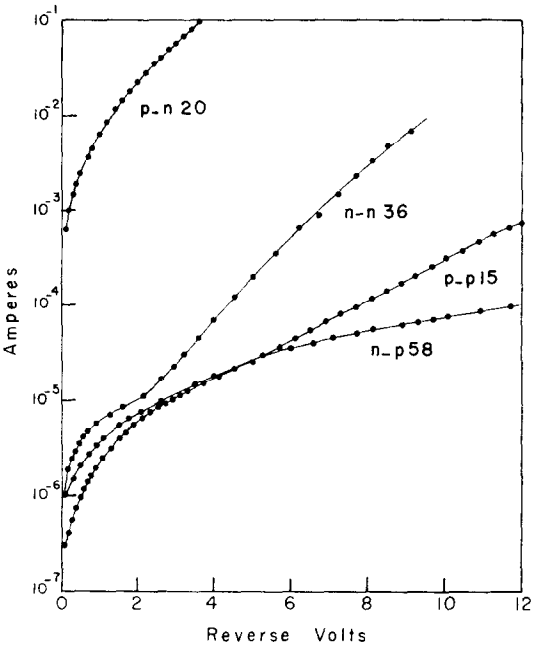

FIG. 12. Reverse I–V characteristic for p–n, n–n, p–p and n–p heterojunction at elevated temperatures. Soft breakdown is observed.

If the interpretation is correct, the small value of transmission coefficient X is a result of the radically different Bloch waves on either side of the interface. For the particular case of the n–n junctions discussed here, if it is assumed that all electrons in the Ge are reflected at the interface except those centered around the $K = (0, 0, 0)$ minimum, and that all these are transmitted, a value of $X = 3 \times 10^{-3}$ results. The actual transmission factor would be expected to be smaller than this because of additional reflection due to the discontinuities in band edges and in the periodicity of the potential-energy function at the interface.

4.3 *Response to monochromatic radiation*

A p–n heterojunction, which the electrical

characteristics suggest has a band profile as in Fig. 5, was illuminated with monochromatic radiation normally incident to the GaAs surface. The resultant photocurrent response is shown in Fig. 13 where the short-circuit photocurrent per

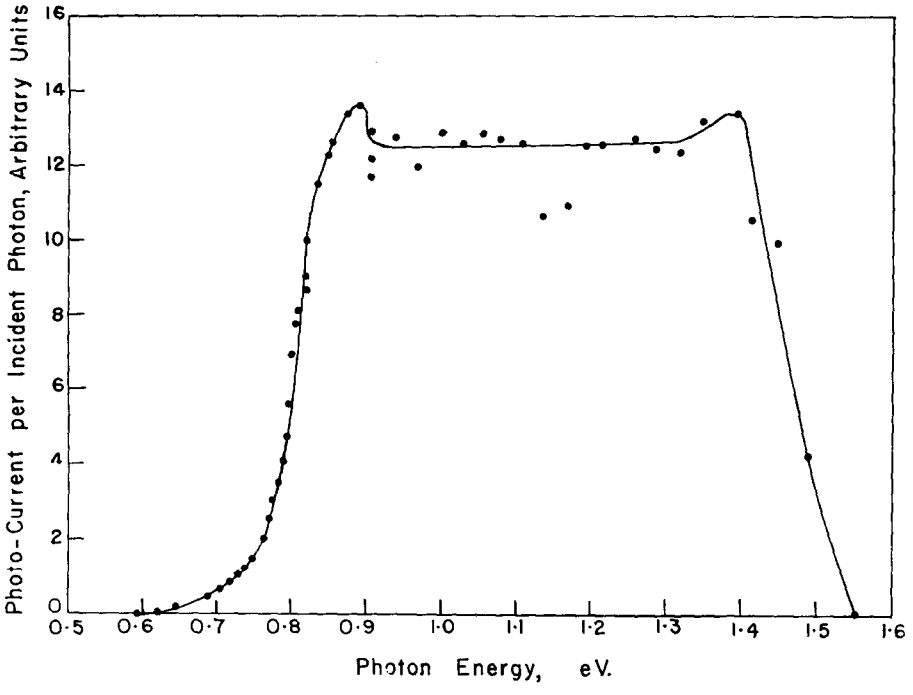

FIG. 13. Short-circuit photocurrent of a p–n heterojunction per incident photon vs. photon energy (see text).

incident photon is plotted against the photon energy.

The response shows a broad maximum between about 0·83 and 1·4 eV. This response may be explained as follows: the higher-energy photons are absorbed near the surface of the GaAs and do not contribute to the photocurrent. However, the GaAs is transparent to photons having energy less than that of the forbidden gap and these photons are transmitted to the interface. These photons having sufficient energy will excite carriers in the Ge and those which excite carriers in the transition region or within a carrier diffusion length of the transition region will contribute to the photocurrent. It is these photons which produce the photocurrent (see Fig. 5). At sufficiently low energy, the photons cannot excite electrons in the Ge and the current is again zero.

It is noticed that both the direct and the indirect absorption edges of the Ge are visible, although the data is not sufficiently accurate to see much "fine structure". The "flat-top" of this figure probably indicates that the incident radiation is entirely utilized in producing photocurrent or else that the absorption coefficient is reasonably constant in this energy range. The decrease to zero in photocurrent in the high-energy region occurs at a value of about 1·55 eV instead of the expected value of the GaAs band gap (1·36 eV). This result is not understood.

5. HETEROJUNCTIONS AS DEVICES

The static I–V characteristics of the diodes studied are in general poorer than obtainable in homojunctions—principally because of the soft reverse breakdown. It is expected that this characteristic may be improved with more work.

An interesting effect in the pulse response is expected from certain heterojunctions. When a diode is abruptly switched from a state of forward bias to a state of reverse bias, no effects on the current due to minority carrier storage are expected. For the n–n and p–p junctions, this is because current is by majority carriers. For p–n and n–p junctions, however, minority-carrier storage exists as in homojunctions. Here, however, the discontinuity at the interface prevents the injected minority carriers from re-entering the GaAs when the diode is abruptly reverse biased.

Preliminary measurements on heterojunctions have detected no effects on the pulse response attributable to storage effects.

A heterojunction can be used as a photocell with a built-in filter, as indicated in Section 4.3. The cell is sensitive for only a narrow band of photon wavelengths.

With the GaAs as emitter, and Ge as base and collector, a wide-gap-emitter transistor seems possible. Such a transistor would be expected to have a high injection efficiency independent of impurity concentration ratio in base and collector. Attempts to construct such a transistor have not been successful.

Although the measurements reported above are on units made from two single depositions of Ge on GaAs, other depositions have been made.

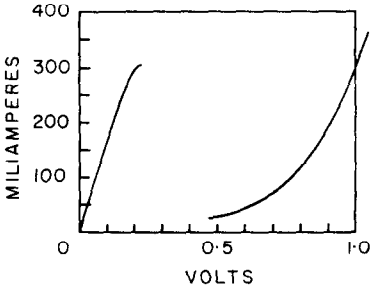

FIG. 14. I–V characteristics of a Ge–GaAs tunnel n–p heterodiode. The ordinate scale is 50 mA/div and the abscissa scale 0·1 V/div.

Degenerate n-type Ge was deposited on degenerate p-type GaAs and diodes were fabricated from this material.* The I–V plots of these units show the typical tunnel-diode characteristic (see Fig. 14). The value of V_D lies between the values obtained in Ge and in GaAs tunnel diodes and is approximately what would be expected from a consideration of the proposed band picture. Fig. 15 depicts the band picture suggested for a tunnel "heterodiode". Tunneling takes place between the Ge conduction band and the GaAs valence band as in tunnel "homodiodes".

The peak-to-valley current ratios for the tunnel heterodiodes at room temperature have been observed to be in excess of 20. Because of the magnitude of the built-in voltage V_D, the valleys are "wider" than the Ge units.

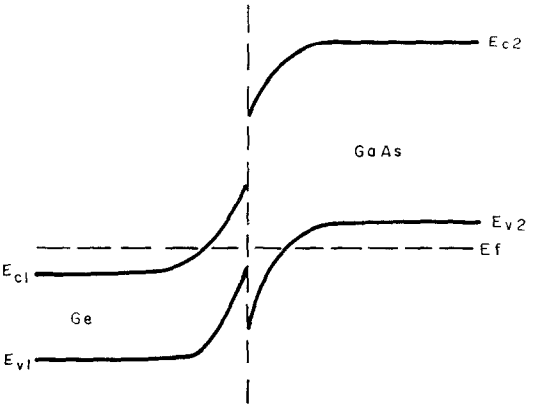

FIG. 15. Energy-band diagram of an n–p tunnel heterodiode at equilibrium.

SUMMARY

Germanium has been deposited on gallium arsenide by a process involving germanium–iodine compounds. The resultant structure is a monocrystal in which the junction between the Ge and GaAs is abrupt.

These junctions rectify. Probing of the junction region shows that the rectification occurs at the interface.

The electrical characteristics of these heterojunctions are roughly what is expected, assuming the conduction and valence band edges are discontinuous at the interface. For the case of degenerate Ge and non-degenerate GaAs, these discontinuities are approximately 0·56 and 0·32 eV respectively. The forbidden band in Ge appears

* This work was carried out by J. C. MARINACE and F. H. DILL.

to move to a region of higher energy as the doping decreases. The discontinuities for non-degenerate Ge and non-degenerate GaAs appear to be 0·15 and 0·55 eV, respectively. There is some evidence, however, which suggests that the discontinuity in conduction band is somewhat larger than this.

All the diodes tested had lower rectification ratios than have available homodiodes. However, unlike the case of homodiodes, no minority-carrier storage effects were observed for these heterojunctions upon switching from a state of forward to reverse bias.

The short-circuit current as a function of input photon energy shows the Ge absorption spectrum.

Tunnel heterodiodes have been fabricated which have I–V characteristics between those of Ge and GaAs tunnel homodiodes.

Acknowledgements—The author wishes to thank Miss ANNE BENORIC of the IBM Corporation, Yorktown Heights, New York, who fabricated most of the heterojunctions for his study. Gratitude is also expressed to J. C. MARINACE, M. J. O'ROURKE, J. A. SWANSON, P. J. PRICE, M. I. NATHAN and W. P. DUMKE for many helpful discussions. The author wishes also to thank J. BALTA-ELÍAS and J. F. GARCÍA DE LA BANDA who made their laboratories at the Consejo Superior de Investigaciones Cientificas (Madrid) available to him, and Professor BARCELÓ for aid in the electro-optical measurements.

REFERENCES

1. See, for example, A. VAN DER ZIEL, *Solid State Physical Electronics* Chaps. 12 and 13. Prentice-Hall, Englewood Cliffs (1957).
2. S. POGANSKI, *Halbleiterprobleme I* (Ed. by W. SCHOTTKY) p. 275. Friedr. Vieweg, Braunschweig (1954).
3. W. SHOCKLEY, *U.S. Pat.* 2,569, 347.
4. H. KRÖMER, *Proc. I.R.E.* **45,** 1535 (1957).
5. D. A. JENNY, *Proc. I.R.E.* **45,** 959 (1957).
6. R. P. RUTH, J. C. MARINACE and W. C. DUNLAP, JR., *J. Appl. Phys.* **31,** 995 (1960).
7. J. C. MARINACE, *IBM J. Res. Dev.* **4,** 248 (1960).
8. R. L. ANDERSON, *IBM J. Res. Dev.* **4,** 283 (1960).
9. A. VAN DER ZIEL, *Solid State Physical Electronics* p. 284. Prentice-Hall, Englewood Cliffs (1957).
10. W. SHOCKLEY, *Bell Syst. Tech. J.* **28,** 235 (1949).
11. H. C. TORREY and C. A. WHITMER, *Crystal Rectifiers.* McGraw-Hill, New York (1948).
12. C. SAH, R. W. NOYCE and W. SHOCKLEY, *Proc. I.R.E.* **45,** 1228 (1957).
13. R. L. ANDERSON and M. J. O'ROURKE, *An. fis. Quim.* **57,** 3 (1961).
14. W. G. SPITZER and J. M. WHELAN, *Phys. Rev.* **114,** 59 (1959).
15. J. I. PANKOVE, *Phys. Rev. Letters* **4,** 454 (1960).